

Modeling of Platinum Clusters in H-Mordenite

Maria E. Grillo* and Maria M. Ramirez de Agudelo

INTEVEP, S.A., Research and Technological Support Center of Petróleos de Venezuela, Apartado 76343, Caracas 1070A-Venezuela, Tel. (58) 2 9088054, Fax (58) 2 9086527 (meg2@intevep.pdv.com)

Received: 5 December 1995 / Accepted: 9 July 1996 / Published: 16 August 1996

Abstract

The size, location and structure of Pt clusters in H-mordenite have been investigated by molecular mechanics energy minimization and molecular dynamics simulation techniques using the **Catalysis** software of Molecular Simulations (MSI). Lattice energy minimizations are performed to study the effects of the specific framework aluminum positions on the location and stability of monoatomic Pt sites in H-mordenite. The lattice energies relative to the siliceous platinum-aluminosilicate structure reveal that the stability of a single Pt atom in H-mordenite is remarkably influenced by the specific location of the Al atoms in the lattice. At the studied Si/Al ratio of two Al ions per unit cell, a stabilization of the H-mordenite lattice upon Pt deposition is obtained. Moreover, lattice energy calculations on Pt/aluminosilicate mordenites of different metal contents per unit cell have been performed. An optimum size for the aggregate confined to the 12-ring main channel that is almost independent of the Pt content per mordenite unit cell has been found. The structural features of the resulting clusters at the end of molecular dynamics simulations on Pt/alumina-mordenites reflect a strong metal-zeolite interaction. The present results are consistent with a previous molecular dynamics simulation study on the structure of platinum deposited on SiO₂ surfaces.

Keyword: Supported Pt clusters, H-mordenite, molecular mechanics, molecular dynamics

Running Title: Modeling of Pt Clusters in H-Mordenite

Introduction

Over the past few years much effort has been given to the study of the catalytic activity of metal/zeolite systems. The activity of this type of catalyst has been related to the dispersion of the metal cluster as well as the nature of the zeolite used. The understanding of the factors controlling the growth process of the metal clusters in zeolite super cages is important for catalyst design. Recently, quite a number of experimental studies have concentrated on understanding and fine tuning the experimental conditions, leading to the most ac-

tive and selective Pt/H-mordenite catalyst. [1-6] This bifunctional catalyst is widely used for hydroisomerization of light alkanes to obtain isomers that have proved to be octane enhancers of gasoline.

The final location and state of the metal ions after the calcination step will determine the final metal dispersion obtained, as suggested by Homeyer and Sachtler. [1] For instance, clusters of a maximum size of 0.8-1.0 nm are obtained in the H-mordenite main channel when suitable preparation conditions are employed. A cluster in this size range is found by Transmission Electron Microscopy (TEM) measurements on H-mordenite, when the platinum amine com-

* To whom correspondence should be addressed

plex $[\text{Pt}(\text{NH}_3)_4]^{2+}$ is calcinated at 300 °C, followed by reduction at 500 °C. [3] Our lattice energy calculations on alumina-mordenites of different Pt contents indicate a maximum cluster size of about 0.8 nm, in agreement with TEM results [3] on Pt/H-mordenite.

In the case of Pt in mordenite, preparation at low reduction temperature, low metal loading and high proton concentration currently result in highly dispersed, even monoatomic, platinum. The monoatomic Pt sites in mordenite were first detected by the H_2 evolution above 300 °C using Temperature-Programmed Desorption (TPD). [4] A later study based on H/D exchange of cyclopentane on Pt/H-mordenite confirms the existence of extremely small Pt particles, possibly monoatomic sites. [5] These isolated Pt atoms are proposed to be located in the side-pockets of the mordenite main channel from the observed stereoselectivity of methylcyclopentane ring-opening catalysis, [4] as well as by Monte Carlo calculations on siliceous mordenite. [7] Furthermore, FTIR studies of CO adsorption suggest that platinum is stabilized by zeolitic protons probably forming $[\text{Pt}_1-\text{H}_2]^{2+}$ adducts. [6] The present calculations demonstrate that the side pocket is the energetically preferred location of a single Pt atom in alumina-mordenite at the considered Si/Al ratio.

The average number of metal atoms per cluster can be estimated by the xenon adsorption method, as developed by Ryoo et al. [8] This method has been used to estimate the cluster size of several group VIII metals supported in cubic faujasite, e.g. Y zeolite, and of Pt in hexagonal faujasite (EMT). [2,8,9,10] A very narrow distribution in the cluster size has been obtained for 2-10 wt% Pt/NaY samples by extended X-ray absorption fine structure (EXAFS) and xenon adsorption measurements. The Pt cluster filling the super cage is proposed to consist of 50-60 atoms. In hexagonal faujasite (EMT), the EXAFS and Xe adsorption results suggest that a Pt cluster of 20-30 atoms is formed in the smaller three windows super cage. An important result of these studies is that the size of the Pt cluster that just fills a super cage does not change with the metal content, and it is stabilized by the interaction with the cage-wall. This is consistent with the present lattice energy calculations and molecular dynamics

Table 1. Interatomic potential parameters of the CVFF_CALP parameter set implemented in Discover. Pt, O, Si and Al refers to the parameters for the platinum atoms and for the oxygen, silicon and aluminum ions in the zeolite structure. The parameters, A_i and B_i , are given in ($\text{kcal/mol}\cdot\text{\AA}^{12}$) and ($\text{kcal/mol}\cdot\text{\AA}^6$), respectively.

i	A_i	B_i
O	272894.7846	498.8788
Si	3149175.0000	710.0000
Al	3784321.4254	11699.8493
Pt	4576819.9618	16963.3082

simulations on $\text{Pt}_x/\text{alumina-mordenites}$, where x is the number of metal atoms per mordenite unit cell.

In this paper the structure and stability of a series of platinum clusters loaded in alumina-mordenite are modeled by both Molecular Mechanics Energy Minimization (MMEM) and Molecular Dynamics Simulations (MDS) techniques. Furthermore, the influence of the specific Al substitution Tetrahedral sites (T-sites) on the location and stability of monoatomic platinum sites in aluminosilicate mordenite is address by using the MMEM procedure.

Methodology

The **Discover** code of MSI [11] was used to perform molecular mechanics energy minimizations (MMEM) and molecular dynamics simulations (MDS) of Pt clusters supported on aluminium substituted at distinct T-sites mordenites. The theoretical aspects and applications of these computational techniques in modeling and predicting crystal structures have been extensively reviewed. [12]

Effects of the Pt content

Molecular Mechanics Energy Minimization. The lattice energy is calculated and minimized using molecular mechanics potential functions (force fields). The functional form of the interatomic potentials implemented in this code include the Coulombic part of the lattice energy calculated exactly by the Ewald summation method and short range forces.

The minimizations are performed in two stages: firstly the aluminosilicate mordenite is relaxed to its minimum energy configuration using a "Consistent Valence Force Field" for the simulation of protonated aluminosilicates included in the **Discover** code (CVFF-CZEO). This force field treats the oxygen atoms as different atom types depending on the particular environment in the aluminosilicate structure and accounts for bridging hydroxyl groups. For a detailed description of the method used to derive the potential parameters as well as the functional form of the potential energy function see references 13 and 14.

In a second stage of the minimization, the energy preferred structure of a Pt cluster inside the aluminosilicate cage is calculated employing a force field implemented in **Discover** which includes metals (CVFF_CALP). This force field accounts for different short-range van der Waals (vdW) forces between the Pt atoms and both Si-O-Si and Si-O-Al sites in the zeolite structure. The potential model used, however, does not contain parameters for the interaction of the zeolitic hydroxyl groups and the Pt atoms. Hence, the present simulations do not account for the polarization effect of the zeolite Brønsted acid sites on the Pt atoms. Nevertheless at the considered Si/Al ratio (two Al ions per unit cell), this omission might not introduce a serious error in determining the effect of the inner zeolite walls interactions with neutral

Table 2. Interatomic potential parameter set, PCFF, implemented in Discover. ϵ_i refers to the potential well depth in kcal/mol, and r_i^* is the interatomic distance in Å.

parameter	r_i^*	ϵ_i
o_z	3.3200	0.2400
a_z	0.0001	0.0000
o_b [a]	5.2191	0.0135
h_b [a]	1.2149	5.2302
o_{sh} [b]	3.4618	0.1591
h_{os} [b]	2.3541	0.0988
o_{as} [c]	5.2591	0.0129
o_{ah} [d]	3.7245	0.1026
h_{oa} [d]	1.2879	3.6860
o_{ss} [e]	3.4506	0.1622

- [a] Oxygen and hydrogen atoms in bridging hydroxyl group.
 - [b] Oxygen and hydrogen atoms in a terminal hydroxyl group connected to silicon.
 - [c] Oxygen atom bonded to aluminum atom.
 - [d] Oxygen and hydrogen atoms in a terminal hydroxyl group connected to aluminum.
 - [e] Oxygen atom between two SiO_4 tetrahedra.
- The pair interaction potential:

$$V(r_{ij}) = \epsilon_{ij} \left[2 \left(\frac{r_{ij}^*}{r_{ij}} \right)^9 - 3 \left(\frac{r_{ij}^*}{r_{ij}} \right)^6 \right]$$

The off-diagonal potential parameters take the form:

$$\epsilon_{ij} = \frac{\sqrt{\epsilon_{ii}\epsilon_{jj}} 2r_{ii}^{*3} r_{jj}^{*3}}{r_{ii}^{*6} + r_{jj}^{*6}}; r_{ij}^* = \left(\frac{r_{ii}^{*6} + r_{jj}^{*6}}{2} \right)^{1/6}$$

Pt atoms, on the structure an stability of large supported clusters.

The metal-zeolite interaction is calculated using a pair Lennard-Jones (12-6) potential:

$$V(r_{ij}) = \frac{A_{ij}}{r_{ij}^{12}} - \frac{B_{ij}}{r_{ij}^6} \quad (1)$$

where r_{ij} is the distance between atoms i and j in angstroms. The off-diagonal, heteronuclear interactions are calculated as geometric averages of the form: $A_{ij} = \sqrt{A_i \times A_j}$ and $B_{ij} = \sqrt{B_i \times B_j}$. The parameters used for the homonuclear

Table 3. Cell parameters and symmetry information on the mordenite lattice. Percent of Al in the tetrahedral sites, $T =$ Tetrahedral. The distances are given in Å

$a = 18.094$ $b = 20.516$ $c = 7.524$ $\alpha = \beta = \gamma = 90^\circ$ space group: Cmc21 (No. 36)			
T1	T2	T3	T4
12	5	28	17

interactions are presented in Table 1. These quantities are related to the potential well depth ϵ_{ij} and with the interatomic distance r_{ij}^* at which the minimum occurs in a straightforward manner:

$$A_{ij} = \epsilon_{ij} r_{ij}^{*12} \text{ and } B_{ij} = 2\epsilon_{ij} r_{ij}^{*6}.$$

The used of a Lennard-Jones potential is a severe approximation in the calculations. However, the success of this approximation in previous studies of the self-diffusion of metallic adsorbates on metallic substrates [15,16,17] and atomic C and O self-diffusion on Pt(111) [18], together with the study of the structural features of platinum deposited on a vitreous silica substrate [19], encourages the used of Lennard-Jones potentials from MSI in this work.

Molecular Dynamics Simulations. The simulation system consists of a single periodically replicated unit cell of H-mordenite containing two aluminium ions, two charge compensating protons and Pt clusters of 20 and 38 atoms per unit cell respectively, $(Pt)_x/H_2Al_2Si_{46}O_{96}$. These structures are previously relaxed to the minimum energy configurations. The equations of motion are integrated with a time step of 0.001 ps in the canonical ensemble (NVT). The system is equilibrated to the desired temperature for 5000 iterations, the dynamics is run for 10000 iterations, equilibrated again for further 5000 iterations and then allowed to converged to a equilibrium structure for 40000 iterations, time over which the measurable properties are averaged. These equilibration and dynamic times proved to be sufficiently long to calculate equilibrium properties of the systems considered.

Effects of the specific Al framework positions

The effect of the position of the Al ions and bridge hydroxyl groups on the location and stability of a single Pt atom in a H-mordenite unit cell is evaluated by MMEM by using a force field potential model, which allows for the interaction

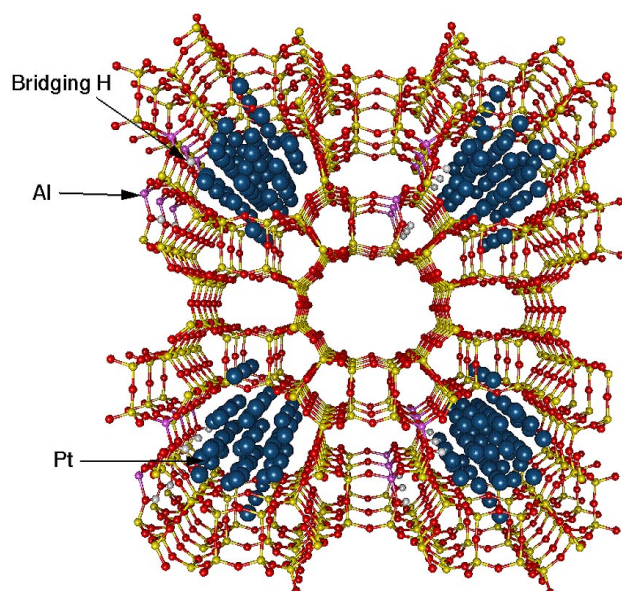


Figure 1. Schematic diagram of the optimum energy structure of the $(Pt)_{22}/H$ -mordenite model system.

of Brønsted acid sites with Pt atoms. For this purpose, a recently released force field (PCFF) accounting for the interaction of Pt with all different atom types in acidic aluminosilicates defined in the CVFF_CZEO parameter set, has been used (see Section 3.2 and Table 2).

Results and Discussion

Effects of the Pt content

Molecular Mechanics Energy Minimizations. The lattice energies of Pt/alumina-mordenites with a metal content ranging from 20 to 40 atoms per unit cell have been calculated. For the purpose of these calculations, we have considered a mordenite unit cell containing two aluminium ions substituted at T1 and T3 sites and two charge compensating protons. For the mordenite structure, the data of Alberti et al., [20] summarized in Table 3 has been used. The framework has four crystallographically distinct T-sites for Si or Al (T = Tetrahedral).

The Pt was introduced as an fcc type cluster in the centre of the unit cell. The minimization proceeds in two steps: first the mordenite framework atomic positions are adjusted until a minimum energy structure is obtained. In a second step of the optimization, the host structure is held rigid and only the Pt atoms are allowed to relax, until a minimum lattice energy is obtained.

In Table 4, the relative lattice energies corresponding to the optimum structures of $(Pt)_x$ /alumina-mordenites with different number of metal atoms, x , per unit cell are given. The calculated energies suggest an optimum cluster size of 23

Table 4. Relative lattice energies, E , in kcal/mol of the considered $(Pt)_n/H_2Al_2Si_{46}O_{96}$ structural models, (Al at T1 and T3 sites). n is the total number of Pt atoms contained per mordenite unit cell. n_{mc} is the number of Pt atoms confined to the 12-ring main channel. Δ is the energy gap between two successive model structures.

model	n	n_{mc}	E^a	Δ
1	20	20	-747.4	
2	22	21	-854.8	-107.4
3	30	22	-1369.1	-514.4
4	34	22	-1641.2	-272.0
5	38	23	-1785.6	-144.4
6	40	24	-1238.6	502.0

[a] Relative to the lattice energy of the siliceous mordenite structure.

atoms located in the 12-ring channel, as a result of the size constraints defined by the cage dimension. This cluster size is nearly independent of the initial number of Pt atoms in the fcc-cluster per unit cell. The remaining Pt atoms are distributed in side pockets. Moreover, the significant energy gap obtained when going from a total Pt content of 38 to 40 atoms per unit cell, is indicative of the maximum metal content per unit cell. Figure 1 shows the resulting structure from the lattice energy minimization of a fcc-type Pt cluster containing 22 atoms per H-mordenite unit cell (model 2).

These results might be related to recent EXAFS and xenon adsorption measurements on 2-10 wt% Pt/NaY and on Pt/EMT zeolites. [10] From these studies it is concluded that the average Pt cluster size in the super cage of NaY zeolite and in the small super cage of EMT is almost independent on the Pt content of the samples.

After the structure optimization, the resulting clusters contained in the mordenite main channel are arranged in a nearly symmetrical manner to just fit the cage dimension. This indicates a significant interaction between Pt and the cage wall, which results in a structure reconstruction of the fcc-metal particles. This metal-zeolite interaction stabilizes an optimum cluster size within the cage and limits the tendency to agglomeration, as suggested by experimental studies on clustering of Pt on FAU types zeolites. [2,10] Moreover, the optimum number of Pt atoms obtained suggests an aggregate of a maximum diameter of 0.8 nm as indicated by TEM results on a Pt/H-mordenite catalysts mentioned above. [3]

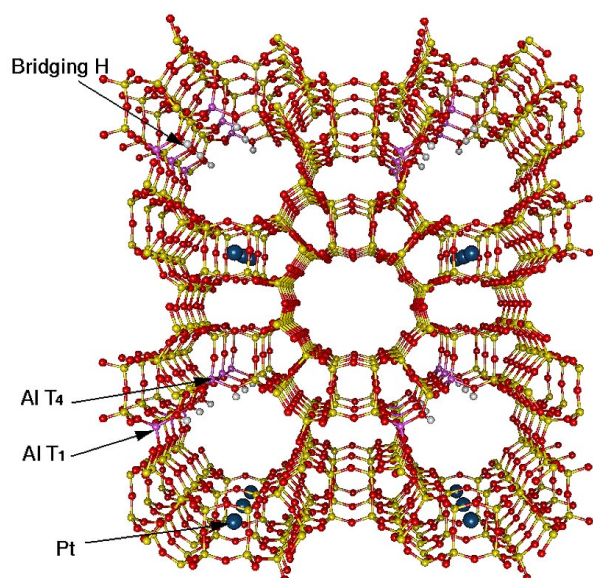


Figure 2. Schematic diagram of the minimum energy Pt location in H-mordenite substituted at the T1 and T4 framework positions.

The strong reconstruction of Pt fcc-clusters induced by the interaction with the zeolite is fully consistent with calculations reported by Levine et al. [19] on structural changes of Pt clusters upon deposition on an amorphous SiO₂ surface. As in the present study, these authors used a pair-wise additive Lennard-Jones (12-6) potential to describe the Pt-substrate interactions. In all simulated deposition processes, low energy Pt clusters resulted to be highly asymmetric and more disorder than in the starting configurations. With increasing the interaction with the surface prior to growth, a corresponding increase in dispersion (smaller particles) was obtained. Moreover conjugate gradient minimizations by Sachdev et al. of isolated Pt clusters with 5-60 atoms with polyhedral symmetry, demonstrated that the non-magic number clusters relaxed into structures which did not resemble the initial polyhedral symmetry. [21]

Molecular Dynamics Simulation results. In this section, Pt/alumina-mordenites of different metal content per unit cell are equilibrated and allowed to relax to an equilibrium structure at 723K. Specifically, the minimized structures 1 and 5 of Table 4 containing 20 and 38 metal atoms per unit cell are taken as starting configurations in the molecular dynamics simulations. The coordination numbers of the nearest Pt-Pt and Pt-O pairs are calculated for a central Pt atom from the corresponding radial distribution functions. The calculated structural features for each of the cluster models are displayed in Table 5.

In both models considered, the metal clusters confined to the 12-ring main channel presents the same average coordination number $N_c^{\text{Pt-Pt}}$ for the nearest Pt-Pt pairs and the bond

Table 5. Calculated structural information for the Pt_n/H-mordenite model structures 1 and 5 ($n=20$ and 38 in Table 4) at 723 K. $N_c^{\text{Pt-Pt}}$ and $N_c^{\text{Pt-O}}$ are the coordination numbers of the nearest Pt-Pt and Pt-O pairs, respectively. $d_{\text{Pt-Pt}}$ and $d_{\text{Pt-O}}$ are the bond lengths in Å for the Pt-Pt and Pt-O pairs, respectively. **fcc** refers to the structure prior to the interaction with the support. **final** refers to the structure after the equilibration at 723 K.

model	5		1	
	fcc	final	fcc	final
$d_{\text{Pt-Pt}}$	2.77	2.66	2.77	2.70
$N_c^{\text{Pt-Pt}}$	12	5	12	5
$d_{\text{Pt-O}}$	1.92	2.78	2.26	2.69
$N_c^{\text{Pt-O}}$	1	3	1	2

length coincides with a range of 2.68 ± 0.2 Å, see Table 5. This also confirms the above mentioned EXAFS results on Pt supported in NaEMT and NaY zeolites. [2,8,10] The calculated $N_c^{\text{Pt-Pt}}$ value for Pt/H-mordenite compares favourably with those from EXAFS for H-mordenite ($N_c^{\text{Pt-Pt}} = 4.2$), [22] NaEMT ($N_c^{\text{Pt-Pt}} = 6.6$) [10] and NaY ($N_c^{\text{Pt-Pt}} = 4.9$). [2] This value is much smaller than the 12 value in the bulk fcc structure indicating an increase in the metal dispersion (smaller particle size) as a result of the size constraint imposed by the cage dimension.

In the resulting clusters of the models 1 and 5, the Pt-O coordination number ($N_c^{\text{Pt-O}}$) increases from 1 (in the fcc-type clusters) to 2 and 3 respectively, see Table 5. This increase of the Pt-O coordination number value indicates a stronger interaction of platinum with the zeolite oxygens in the low energy structure compare to the initial configuration. The metal redispersion is higher for the Pt cluster model 5 ($n=38$). A decrease in the coordination number might be seen as a decrease in dimensionality of the Pt crystals, similar to that found by Levine et al. for Pt deposition on SiO₂ surfaces (as shown in Fig. 1). A decrease in $N_c^{\text{Pt-Pt}}$ from 12 in the fcc particles to a cluster of $N_c^{\text{Pt-Pt}} = 5$ might suggest a change from tridimensional particles to almost bidimensional ones. Thus, this might predict the growth of flakes or even ribbon-type crystals attached and stabilized by the zeolite walls.

Effects of the specific Al framework positions

The framework stability of mordenite containing two aluminium ions, one Pt atom and two charge compensating protons per unit cell has been studied by means of Molecular Mechanics Energy Minimizations (MMEM). In this section,

Table 6. Relative lattice energies, E , in kcal/mol of the six calculated Pt/H-mordenite structural models, (Pt/ $H_2Al_2Si_{46}O_{96}$). Δ is the energy difference between two successive models.

model	Al T-sites	E [a]	Δ	Pt location
1	T1, T4	-293.3	8.5	s.p.
2	T3, T4	-284.79	6.9	s.p.
3	T2, T4	-277.88	3.2	s.p.
4	T1, T3	-274.73	14.4	m.c.
5	T1, T2	-260.31	4.1	m.c.
6	T3, T2	-256.25		m.c.

s.p.: side pocket

m.c.: main channel.

[a] Relative to the lattice energy of the siliceous Pt/mordenite structure.

we concentrate on the effects of the specific location of the two Al atoms within the mordenite framework on the stability of the Pt/aluminosilicate mordenite lattice. It is assumed that the specific locations of the bridging hydroxyl groups within the mordenite lattice have only a secondary effect on the lattice stability. This is based on recent lattice energy calculations on H-mordenite, which report that there is not a single preferred bridging hydroxyl group. Instead, these are found to be distributed over several framework sites. [23] Hence, in this work the two OH groups are distributed over arbitrary chosen lattice sites.

The six possible structural models, combining two Al ions substituted over the four crystallographically different T-sites in the mordenite lattice have been calculated. In all the structures considered, the Pt atom was initially located at the centre of the 12-ring main channel. The effect upon aluminium insertion in the siliceous Pt/mordenite structure is a stabilization of the lattice energy (more negative). In Table 6, the lattice energies of the calculated Pt/H-mordenite structural models relative to siliceous Pt/mordenite are displayed. As reflected by the energy difference between successive models, the position of the Al ions within the framework structure influences significantly the lattice stability of Pt loaded in H-mordenite.

In the three most energetically favoured structural models of Pt/H-mordenite (see Table 6) as well as in the siliceous structure, the minimum energy configuration locates the Pt atom in side pockets. This suggest that at the Si/Al ratio stud-

ied, the preferred Pt location is determined by the more effective dispersive vdW interactions in a smaller pore.

Considering the experimental enrichment of Al in the mordenite T-sites (see Table 3), the obtained trend in relative stabilities of Pt/H-mordenites (see Table 6) indicates that for an alumina-mordenite with aluminium statistically distributed throughout the structure, there is a high probability of finding Pt nucleation sites in side pockets. Obviously, in real cases that would depend on the pretreatment temperatures to which the solid has been subjected.

This result has already been suggested by the stereoselectivity of the methylcyclopentane conversion catalysis on Pt/H-mordenite [4] and predicted by a previous Monte Carlo simulation study of Pt on siliceous mordenite. [6] This might also be related to the formation mechanism suggested by Sachtler et al. for transition metal clusters (Pt, Pd and Ni) in NaY zeolite at high calcination temperatures. In the proposed kinetic path, the bare metal ions migrate after calcination to smaller cages that provide greater charge stabilization. [1]

Upon deposition of a Pt atom on acidic mordenite, a stabilization of all six structural models with respect to the H-mordenite lattice was obtained. The largest stabilization on Pt loading of -17.8 kcal/mol was obtained for the H-mordenite with the Al atoms substituted in the framework positions T1 and T3 (model 4 in table 6). An energy lowering of about 16 kcal/mol was obtained for all structural models involving the T4 Al-substitution site (first three low energy structures in Table 6).

Conclusions

The present lattice energy minimization results suggest that the relative stability of monoatomic platinum sites in aluminosilicate mordenites is related to the specific aluminium insertion T-sites in the framework structure. Nevertheless at the Si/Al ratio studied, the optimum Pt location is determined by the interaction with mordenite walls rather than by the interaction with Brønsted protons, as observed by the calculated effect of aluminium substitution on platinum location in mordenite (see Table 6).

Lattice energy minimizations and molecular dynamics simulations on Pt/alumina-mordenites of different Pt contents seem to indicate that the structural features of the platinum cluster confined to the 12-ring main channel are almost independent of the total Pt content, and strongly dependent upon the surrounding zeolite structural field.

References

1. Homeyer, S. T.; Sachtler, W. M. H. in *Stud. Surf. Sci. Catal.*; Weitkamp, J.; Karge, H.G.; Pfeifer, H., Hölderich, W. (Eds.) Elsevier: Amsterdam, 1989; Vol. 49, pp 984-975.

2. Ryoo, R.; Cho, S. J.; Pak, C.; Lee, J. Y. *Catal. Lett.* **1993**, *20*, 107.
3. Giannetto, G.; Montes, A.; Alvarez, F.; Guisnet, M. *Revista Soc. Venez. Catal.* **1991**, *5*, 33.
4. Lerner, B. A.; Carvill, B. T.; Sachtler, W. M. H. *J. Mol. Catal.* **1992**, *77*, 99.
5. Lei, G.; Sachtler, W. M. H. *J. Catal.* **1993**, *140*, 601.
6. Zholobenko, V.; Carvill, B.; Lerner, B.; Lei, G.; Sachler, W. M. H. *Proceedings of the 206th National Meeting American Society*, Chicago, IL, **1993**, 735.
7. Blanco, F.; Urbina-Villalba, G.; Ramirez de Agudelo, M. M. in *Stud. Surf. Sci. Catal.*; Weitkamp, J.; Karge, H. G.; Pfeifer, H.; Hölderich, W. (Eds.) Elsevier: Amsterdam, 1994; Vol. 84, pp 2162-2155.
8. Ryoo, R.; Cho, S. J.; Pak, C.; Kim, J-G; Ihm, S-K; Lee, J. Y. *J. Am. Chem. Soc.* **1992**, *114*, 76.
9. Kim, J-G; Ihm, S-K; Lee, J. Y.; Ryoo, R. *J. Phys. Chem.* **1991**, *95*, 8546.
10. Ihee, H.; Bécue, T.; Ryoo, R.; Potvin, C.; Manoli, J-M; Djéga-Mariadassou, G. in *Stud. Surf. Sci. Catal.*; Weitkamp, J.; Karge, H. G.; Pfeifer, H.; Hölderich, W. (Eds.) Elsevier: Amsterdam, 1994; Vol. 84, pp 772-765.
11. Discover Molecular Simulation Program, version 94.1, Molecular Simulations Inc., San Diego, 1995.
12. Catlow, C. R. A. *Modelling of Structure and Reactivity in Zeolites*; Academic Press: London, 1992.
13. Hill, J-R; Sauer, J. *J. Phys. Chem.* **1994**, *98*, 1238.
14. Hill, J-R; Sauer, J. *J. Phys. Chem.* **1995**, *99*, 9536.
15. Doll, J. D. and McDowell, H. K. *J. Chem. Phys.* **1982**, *77*, 479.
16. Doll, J. D. and McDowell, H. K. *Surf. Sci.* **1983**, *123*, 99.
17. McDowell, H. K. and Doll, J. D. *J. Chem. Phys.* **1983**, *78*, 3219.
18. Doll, J. D.; Freeman, D. L. *Surf. Sci.* **1983**, *134*, 769.
19. Levine, S. M.; Garofalini, S. H. *Surf. Sci.* **1985**, *163*, 59.
20. Alberti, A.; Davoli, P.; Vezzalini, G. *Z. Kryst.* **1986**, *175*, 249.
21. Sachdev, A.; Masel, R. I.; Adams, J. B. *J. of Cat.* **1992**, *136*, 320.
22. Lamb, H. H.; Clayton, M. J.; Otten, M. M.; Reifsnnyder, S. N. Presented at the 14th North-American Meeting of the Catalysis Society, Snowbird, Utah. June 11-16, 1995.
23. Schöder, K-P; Sauer, J. *Proceedings of the 9th International Zeolite Conference*, Montreal 1992; von Ballmoos, R., et al. (Eds.) Butterworth-Heinemann, 1993; pp 694-687.